INTERNATIONAL JOURNAL OF ENERGY STUDIES

e-ISSN: 2717-7513 (ONLINE); homepage: https://dergipark.org.tr/en/pub/ijes

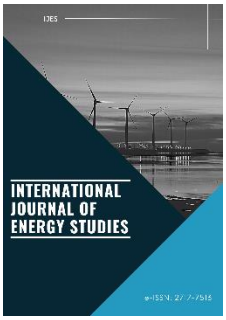

Research Article

Int J Energy Studies 2024; 9(1): 69-92

DOI: 10.58559/ijes.1426354

Received : 26 Jan 2024

Revised : 06 Feb 2024

Accepted : 02 Mar 2024

Design and optimization of battery and thermal management system for AC photovoltaic energy module

Sahin Gullu[a*], Issa Batarseh[b], Fahad Alaql[c]

[a]University of Central Florida, Department of Electrical and Computer Engineering, ORCID: 0000-0002-2997-172X

[b]University of Central Florida, Department of Electrical and Computer Engineering, ORCID: 0000-0002-8420-1891

[c]Imam Mohammad Ibn Saud Islamic University, Department of Electrical Engineering, ORCID: 0000-0003-0178-0232

*(*Corresponding Author: sahin.gullu@ucf.edu)*

Highlights

- The techno-economic impact of AC-PV system is analyzed.
- Optimum battery capacity size and PV panel size is calculated.
- Battery electrical model, battery thermal model, and PV themperature model are designed.
- Battery cell tests are performed in order to obtain battery electrical model parameters.

You can cite this article as: Gullu S, Batarseh I, Alaql F. Design and optimization of battery and thermal management system for AC photovoltaic energy module. Int J Energy Studies 2024; 9(1): 69-92.

ABSTRACT

The utilization of renewable energy sources has increased due to concerns about climate change. However, injecting the power from renewable energy sources into grid-tied systems is challenging. The techno-economic analysis a photovoltaic (PV) energy systems is investigated. As a result, this paper presents AC-PV module for Grid-Tied and Off-Grid Scenarios via optimization, modeling, and test results. Even though the output of a PV panel is DC voltage, a three-port inverter and a lithium-ion battery pack are integrated with the back of the PV panel. They are packaged as a PV system module that makes the module output have AC voltage. Therefore, an optimized AC-PV module can be a solution for residential and commercial use, which are grid-tied systems; it can be very efficient for those without access to electricity, which is an off-grid system. An integrated battery and thermal management strategy is crucial for this AC-PV module. In the article, the battery capacity optimization, the electrical and the thermal model of the battery pack, battery heat generation model are discussed by using stochastic analysis techniques; the battery test results are also obtained to identify the models' parameters and a control algorithm is proposed to extract the battery information such as temperature, current, voltage, SoC and SoH of the battery pack.

Keywords: Battery management system, Battery model, Lithium-ion battery, Photovoltaic systems, Thermal management system

1. INTRODUCTION

Energy access is one of the main challenges in the world due to the fact that energy is the center of our life. As a result, it affects a region's agriculture, education, health, and economy. Today, three billion people are in lack of energy, and more than one billion people are not able to access electricity [1]. Generating electricity from PV panels and storing that energy can help people to have the basic life necessities for an off-grid scenario. Also, other main challenges are to generate clean energy and to send that energy to the traditional electric grid by using grid-forming (GFM) inverters to maintain a healthy grid-tied system. Today in the market, most inverters are grid-following (GFL) inverters, which are called current controlled inverters. They resembles a current source. GFL inverters could be defined as grid-supporting or grid-feeding inverters. Grid-supporting inverters are usually used in large-scale inverter-based resources (IBRs) such as above 5 MW. Grid-supporting inverters supply reactive power and varying active power at predefined droop setting [2]. Grid-feeding inverters maintain a constant current output and provide active power in phase with the grid because they focus on MPPT and zero reactive power [3,4].

Therefore, integrating PV, inverter and energy storage as an AC-PV module might help solve this energy problem. This modular design can also be used for grid-tied scenarios in rural areas or cities to help people use clean energy to decrease carbon emissions. Moreover, it may help the utility during the high demand for electricity if it has access to customers' energy storage. The integration of the PV-battery-inverter module is a relatively new concept, as shown in Figure 1, and this integration interest has been mainly directed at low-power applications [5]. However, these developed ideas are tended to be ineffective due to the lack of battery charging and discharging schemes, and battery management systems [6]. Even though the concept of integrating PV, inverter and battery pack can be a solution, its feasibility and system analysis must be addressed. Therefore, a battery and thermal management system (BTMS) for this AC-PV module are discussed in this article to establish the optimal protection of the module.

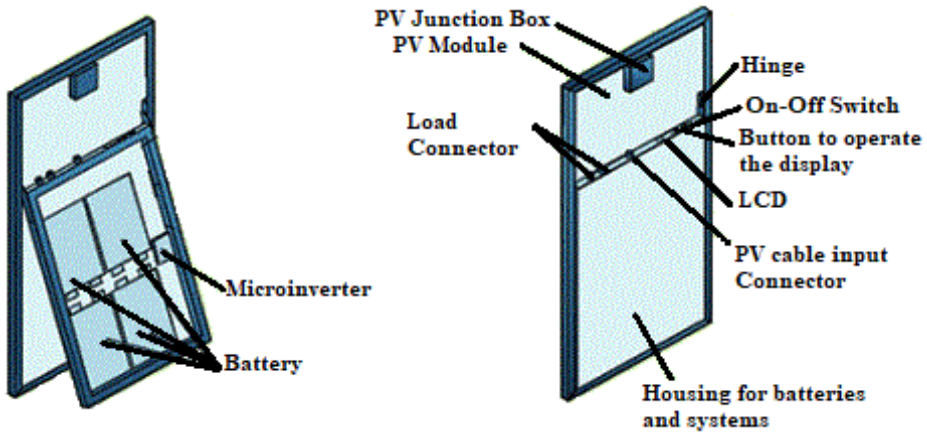

Figure 1. AC-PV module

The conventional battery management system (BMS) feature usually estimates the State of Charge (SoC) to protect the batteries [7-9], but it is not enough for safety issues. Even though SoC gives the user how long the batteries can be utilized, other parameters are also needed, such as voltage, charging-discharging current, temperature, and State of Health (SoH), to have a complete battery management system. Moreover, although some BMSs provide SoH, they do not provide a thermal management techniques [10-12]. The purpose of BTMS, which is called intelligent BMS (i-BMS) in this paper, is to eliminate safety issues and thermal runaway by obtaining the optimal size of the battery pack, the battery pack's electrical & thermal model, and the thermal analysis of the system. Terefore, this BTMS differs from conventional BMS. Also, depending on applications, the three-port biderctional inverter in Figure 1 might be changed by a multiport inverter. Multiport inverters can be single-stage inverters [13,14] or dual-stage inverters [15,16] that consist of multiple converters' integration.

The objective of this article is to demonstrate the feasibility of this concept. Figure 2 shows two main parts in i-BMS are discussed: Battery pack size and Battery Electrical & Thermal Model. They are optimizing the battery pack capacity and modeling the battery pack variables to control the temperature and estimate the SoC and SoH of the battery pack. In Section II, the models of AC-PV module are designed. Section III shows the algorithm [17] that determines the optimum battery capacity for a AC-PV module. Section IV includes the test results and a discussion of the parameter identification of battery models. Finally, in Section V, a brief conclusion is presented.

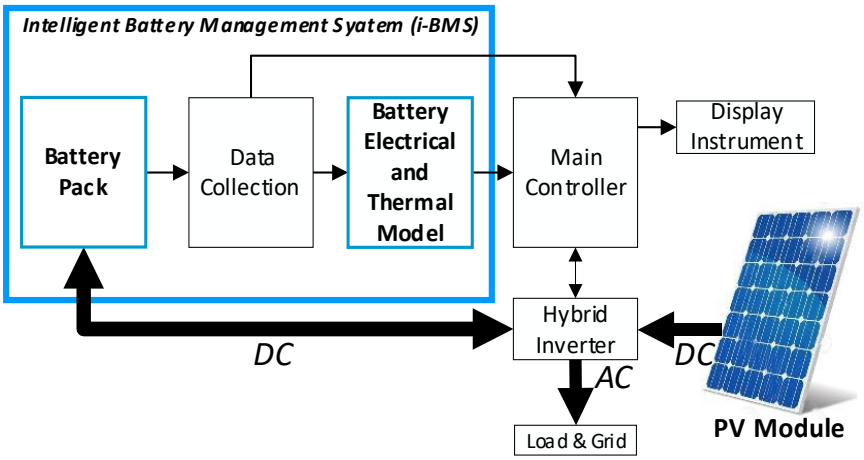

Figure 2. Block diagram for AC-PV module that focuses on the battery pack, battery models and battery management systems

2. DESIGNING MODELS

The bottleneck in AC-PV module is the batteries' temperature. The first cause that affects the temperature of the module and the batteries is the Sun. Since the battery parameters depend on the temperature such as the voltage and internal resistance of batteries, it changes the accuracy of SoC, and SoH. Also, the sensors outputs highly rely on the temperature variations, i-BMS is required to overcome this temperature issue first. Figure 3 shows the block diagrams of how the main controller provides output based on the information from the battery pack and battery models. Three models are discussed in this section, as seen in Figure 3 their texts are bolded. They are battery electrical model, PV panel temperature model, and battery thermal model.

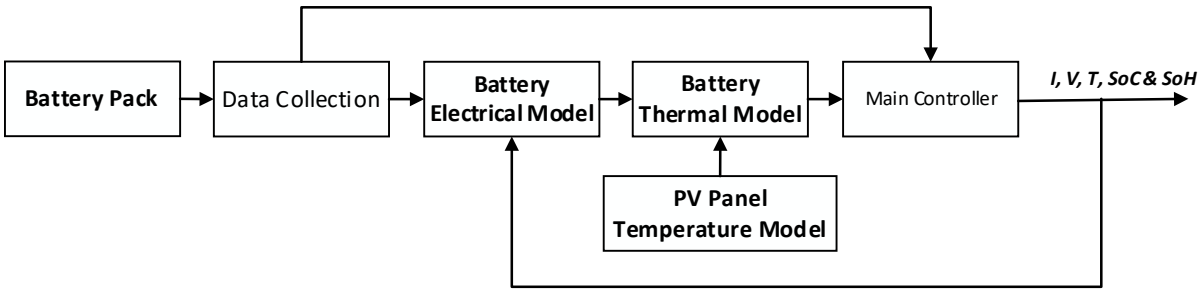

Figure 3. Battery parameters estimation block diagram

2.1. Battery Electrical Model

The first model discussed in this section is the battery electrical model. Two models applied to batteries in the literature are the Electrochemical Model and Equivalent Circuit Model (ECM). The Electrochemical Model utilizes the internal reaction of batteries, whereas ECM emphasizes the external characteristic of batteries. The Electrochemical model is more accurate for age modeling; however, the chemical reactions, nonlinearity, and time-varying parameters inside the batteries are complex and challenging to determine. Because of that, ECM, shown in Figure 4a, is usually preferred to be used, and it is easy to implement for electrical engineers. Parallel RC circuits demonstrate the behavior of batteries during charge/discharge. Depending on the number of RC circuits, the names are defined as Linear (zero RC circuits), Thevenin (one RC circuit), and the Dual polarization model (two RC circuits). Reference [18] compares ECMs circuits, and when the computation time and the voltage error are considered, the optimal solution is to use the Thevenin model illustrated in Figure 4b.

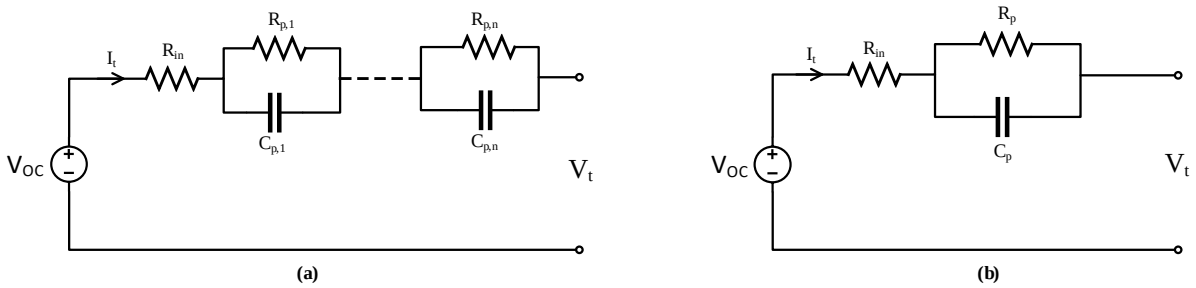

Figure 4. (a) General form of ECM; (b) Thevenin model

Equation (1) is governed by the Thevenin model, and the initial voltage drop of the RC circuit is zero. Therefore, the terminal voltage of a cell is expressed in Equation 3 in case of discharge (it can be applied in case of charge). SoC is estimated from the Ampere-hour formula as described in Equation 4. SoC is a short-time variable compared to SoH, so that SoH is calculated in Equation 5 after saving the SoC data.

$$V_T(t) = V_{OC} - I_T(t) \cdot R_{in} - V_P(t) \tag{1}$$

$$V_P(t) = V_P(0) \cdot e^{-\frac{t}{R_P C_P}} + \int_0^t \frac{1}{C_P} \cdot I_T(x) \cdot e^{-\frac{x}{R_P C_P}} \cdot dx \tag{2}$$

$$V_T(t) = V_{OC} - I_T(t) \cdot R_{in} - \left(1 - e^{-\frac{t}{\tau_P}}\right) \cdot I_T(t) \cdot R_P \quad (3)$$

$$SoC(t) = SoC(t_0) - \frac{\int_{t_0}^{t} \eta_{batt} \cdot I_T(x) \cdot dx}{SoH_{max}} \quad (4)$$

$$SoH(t) = \frac{\int_{t_0}^{t} \eta_{batt} \cdot I_T(x) \cdot dx}{SoC(t) - SoC(t_0)} \quad (5)$$

2.2. PV Panel Temperature Model

The battery pack's heat is primarily because of the effect of the Sun because the charging and discharging currents are limited that does not increase the battery cells temperature. However, the heat due to the charging and discharging is discussed in the next section.

During the day, the PV panel's temperature increases; so this affects the battery pack. Based on Figure 5, Equation 6 can be derived from the energy balance theory. In Equation 7, the heat flux (q_s) from the solar irradiance is equal to the multiplication of the solar energy absorption rate and solar irradiance. Also, the power flux of electrical energy (q_e) depends on solar irradiance and photoelectric efficiency of solar cells, as shown in Equation 8. Equation 9 and Equation 10 point out the heat dissipation (q_c & q_r) by convection and radiation, which depend on the temperature of the PV panel and the weather.

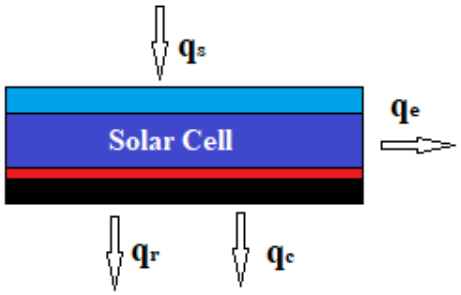

Figure 5. 1-D PV panel temperature model

$$q_s = q_c + q_r + q_e \quad (6)$$

$$q_s = e_0 \cdot Q_s \quad (7)$$

$$q_e = \beta \cdot Q_s \tag{8}$$

$$q_c = 2h_c \cdot (T_{PV} - T_w) \tag{9}$$

$$q_r = 2e_1\sigma_{sb} \cdot ({T^4}_{PV} - {T^4}_w) \tag{10}$$

Equation 11 is derived by using Equation 6, 7, 8, 9 and 10. As seen in Equation 11, the PV panel temperature can be found numerically. However, Ref. [19] suggests an equation for a realistic model in Equation 13.

$$T_{PV} = \frac{Q_s \cdot (e_0 - \beta) - 2e_1\sigma_{sb} \cdot ({T^4}_{PV} - {T^4}_w)}{2h_c} + T_w \tag{11}$$

$$h_c = 2.8 + 3.8 \cdot v_{wind} \tag{12}$$

$$T_{PV} = \frac{Q_s \cdot (e_0 - \beta)}{(1 + \alpha) \cdot (2.8 + 3.8 \cdot v_{wind})} + T_w \tag{13}$$

The temperature of the PV panel determines the ambient temperature inside the AC-PV module; this affects the battery pack's thermal strategy. When the AC-PV module is designed, the worst-case scenario must be applied. Therefore, the AC-PV module's temperature range must be found to decide the optimal thermal strategy. That is why the passive and active thermal management strategies and battery thermal models are reviewed in the next section.

2.3. Battery Thermal Model

Active cooling and heating systems are mostly air, liquid, refrigerant, and thermo-electric module, whereas passive thermal systems can be air, phase change material (PCM), and heat pipe. When active air cooling is not integrated, this strategy cannot control the temperature in an acceptable range [20]. The temperature uniformity between battery cells is not achieved, which can lead to thermal runaways. Liquid cooling needs a recycling unit that adds complexity, weight, and high-power consumption compared to an air cooling system, although it has better heat capacity and thermal conductivity [21]. The refrigerant is a subcategory of the liquid cooling system, and it has

higher power consumption than liquid one due to additional components. Among the active cooling system, the thermo-electric module is inefficient because of its small contact area and high cost; it also requires power support [22]. While heat pipe technology is passive, it can be challenging to incorporate due to its bulky condenser and evaporator sections. Additionally, it is not advisable to use it alone in high-temperature situations unless it is combined with an air cooling system [23].

Another passive cooling technique is PCM which changes its phase when it absorbs/releases energy. PCC is a form of PCM, and it is implemented in battery packs. Its melting point is usually 55^0 C [24]. PCC has the ability to reduce the temperature difference between lithium-ion cells and make it more uniform [25, 26], Figure 6 shows and example of PCM usage in real-world application. Additionally, it can help to reduce the impact on the batteries. PCC can also provide heating for the battery pack at night, which absorbs energy during the day. Since the battery's heat is not usually due to the high charging or discharging current, covering the back of the PV cells with PCM also reduces the temperature of the batteries and the whole system. Reference [27] states that PV cells' temperature dropped by 35 °C with 2 cm PCM layer thickness by using a computer model. Therefore, PCC can tolerate the temperature of a PV panel until it reaches 90^0 C.

Figure 6. PCM usage in a battery pack (Courtesy of Beam Global [28])

Table I provides a comparison of various thermal management techniques for the purpose of enhancing comprehension. This AC-PV module is a mobile system, so it must be lightweight. It must be cost-effective and efficient to be commercialized. These parameters help us to obtain PCM on the back of the PV panel and PCC around the battery cells. It is a reasonable and optimized solution as a thermal management system in the module.

Table 1. Comparison of thermal management techniques

Thermal System	Weight	Power Consumption	Cost	Efficiency
Air	Moderate	Low	Moderate	Low
Liquid	High	Moderate	High	High
Refrigerant	Moderate	High	High	High
PCM	Moderate	No	Moderate	Moderate
Heat pipe	High	No	Moderate	Moderate
Thermo-electric	Moderate	Moderate	High	Low

The battery pack is composed of modules, which means that the internal resistance of the each battery cells could be a reason for any thermal changes that affect the battery module's thermal model. This irreversible heat generation is expressed in Equation 14.

$$Q_{cell} = I_T \cdot (V_T - V_{OC}) \tag{14}$$

$$C_c \cdot \frac{dT_{cell}}{dt} = \frac{T_a - T_{cell}}{R_c} + Q_{cell} \tag{15}$$

The cell thermal model is shown in Figure 7, and the equation is expressed in Equation 15. The battery module includes 12 lithium-ion cells in series (LG MH1 18650 cylindrical with 3.2 Ah capacity and 3.67 V). The on-board temperature estimation is crucial for the feasibility and safety of the AC-PV module. Thus, the battery thermal model is enforced to estimate the temperature of each battery cells and the battery pack.

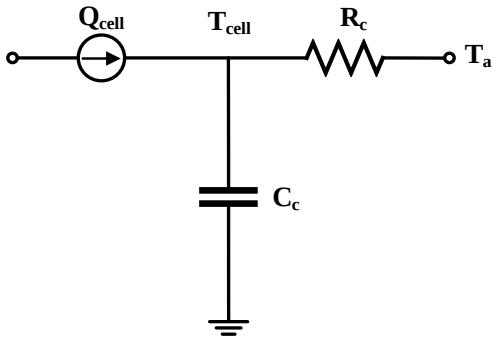

Figure 7. Cell equivalent circuit thermal model

3. OPTIMIZATION

In this section of the article, the models defined in previous section are optimized to determine the model parameters.

3.1. Determination of PV Panel and Battery Size

To calculate the optimal capacity of a battery pack for each PV panel, the following parameters are required: the irradiance of the location for one year, the load profile of the location for one year, the power rating of the PV panel, the efficiency of the three-port inverter, the efficiency of the battery pack during charging & discharging, the desired minimum and maximum SoC, the cost of PV panel per watt, the cost of lithium-ion battery per watt-hour.

In a given present time t, the following parameters are calculated: the generated total power from PV panels at time t in Equation 16, $P_{gen}(t)$, is the multiplication of one PV panel power and the total number of PV Panels. The total power stored at time t in the battery shown in Equation 17 depends on the power stored in the battery in the previous time interval, the total generated power at time t, the load power at time t, the three-port inverter efficiency, and the efficiency of the battery pack during discharging or charging. The desired total energy in the battery pack at time t is expressed in Equation 18.

$$P_{gen}(t) = P_{PV}(t) \cdot N_{PV} \tag{16}$$

$$P_b(t) = P_b(t-1) + \left(P_{gen}(t) - \frac{P_l(t)}{\eta_{inv}}\right) \cdot \eta_{batt} \tag{17}$$

$$E_{b,min} < E_b < E_{b,max} \tag{18}$$

$E_{b,min}(t)$ and $E_{b,max}(t)$ are the minimum and maximum total energy stored in the battery pack. They are calculated from the nominal battery energy mentioned in Equations 19 and 20. SoC_{min} and SoC_{max} are defined as desired minimum and maximum state-of-charge.

$$E_{b,min}(t) = SoC_{min} \cdot E_b \tag{19}$$

$$E_{b,max}(t) = SoC_{max} \cdot E_b \tag{20}$$

When the power generated from PV panels and the power stored in the battery pack are not enough to cover the load power at time *t*, the Loss of Power (ΔP_{LP}) is defined in Equation 21 as:

$$\Delta P_{LP}(t) = P_L(t) - \left(P_{gen}(t) + P_b(t-1) - P_{b,min}(t)\right) \cdot \eta_{inv} \tag{21}$$

As it can be extracted in Equation 21, the power loss occurred when ΔP_{LP} is positive. As a result of that, the deficient amount of power is taken from the grid. When ΔP_{LP} is negative at time *t*, it shows that there is surplus power. That excess power is sent to Grid if the battery's total energy reaches the maximum SoC. The power management scenarios illustrated in Figure 8 are encoded to ascertain the optimum size of the PV panels power rating and the capacity of batteries. The power management algorithm scenarios are explained for better understanding as follows:

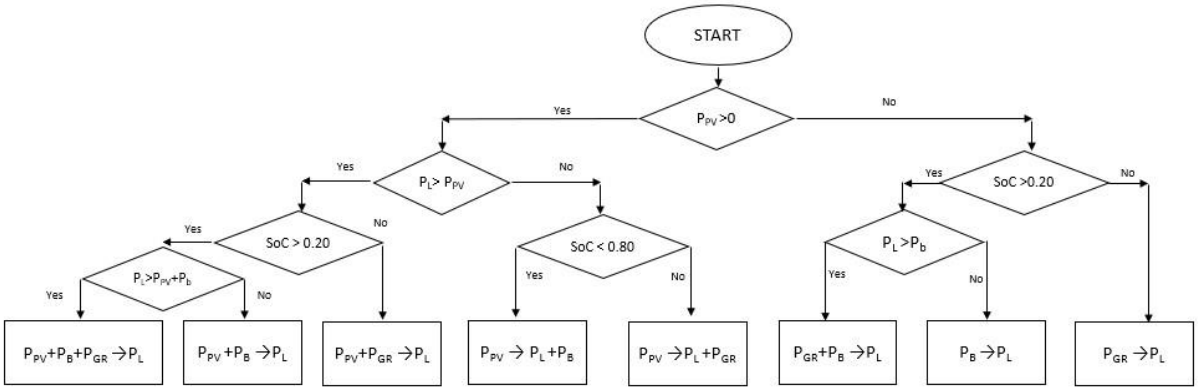

Figure 8. Power management block diagram

All the power flow scenarios start with checking the PV panels power whether it is available or not. Then it checks how much power the load requires. After that, the code examines how much the battery pack's energy is available. As a conclusion, it decides how load power is compensated by the supply sources. It should be mentioned that P_{PV} is a power source, P_L is a load; however, P_b and P_{GR} can be source or a load depending on the situation. Therefore, it is very critical to make a correct decision which case is occurring in the AC-PV module.

1. If PV panels produce power. However, the power from the PV panels are enough for the load. Then, if the batteries do not have enough energy to cover Load power, then the

remaining power is taken from Grid. Therefore, all the power sources are combined to meet Load power.

2. In this case, after checking the PV panels' power and the SoC of the battery pack, it is concluded that the power from Grid is not needed.
3. If PV panels are not producing sufficient power and the battery packs' SoC is lower than the desired level, the PV panels and Grid are used to provide power to Load.
4. The PV panels are supplying adequate power to the load, then there is extra power remaining. That power is sent to the batteries if the batteries' SoC is lower than the maximum SoC.
5. If there is an excess power from the PV panels as described in previous case and the battery is reached its maximum SoC, then that power is directed to Grid .
6. In this case, the PV panels do not have power produced. Therefore, the load takes power from Grid and the batteries when the batteries' SoC is higher than the minimum SoC.
7. The battery energy is solely utilized in this case because PV is off, and Grid is not needed.
8. The Sun is below the horizon, and the batteries' SoC hits 0.2; therefore, Grid supplies the power for Load.

The goal is to make the power taken from Grid and the power sent to Grid equal, which means that the net power should be zero. In grid-tied case, the customer's electric payment is aimed to be zero at the end of the year. In off-grid scenario, there should not be the Loss of Power. Therefore, the Net Power Probability (NPP) is defined in Equation 22 as the ratio of the total power loss to the total load power.

$$NPP = \frac{\sum_{t=1}^{T} \Delta P_{PL}(t)}{\sum_{t=1}^{T} P_L(t)} \tag{22}$$

The total cost in Equation 23 is defined as the sum of the PV panel cost, the battery pack cost, and other costs such as cables, packaging, insulation material, and inverter costs. The additional costs can be considered equal for each AC-PV module. The slope in Equation 24 depends on the cost of the battery ($/Wh) and the cost of the PV panel ($/W).

$$C_{total} = C_{pv} + C_{battery} + C_{other} \tag{23}$$

$$C_{total} = a \cdot P_{pv} + b \cdot E_{battery} + C_{other} \quad (24)$$

In our design, the irradiance data and load profile data are shown in Figure 9 and Figure 10, respectively, for Orlando. The solar panel is an ASP-390M, which has 0.39 kW output power. The three-port inverter's efficiency is 0.98, the lithium-ion battery efficiency differs during charging and discharging, also its efficiency goes down over time. Therefore, the worst case scenario is 0.90, and desired minimum and maximum SoC are 0.2 and 0.8. The lithium-ion battery and PV Panel costs are 0.4 $/Wh and 0.34 $/W, respectively [29,30].

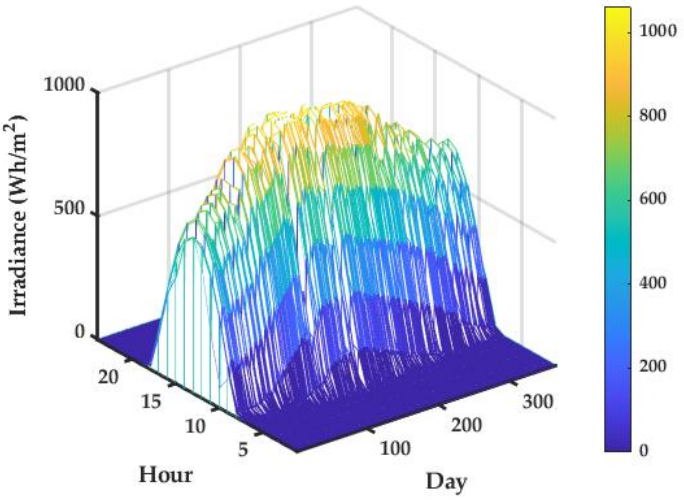

Figure 9. Average monthly solar irradiance in Orlando

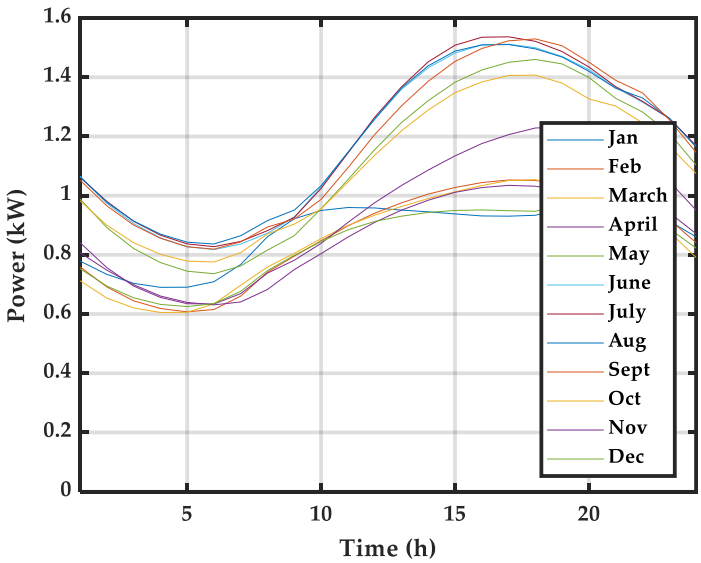

Figure 10. Average power demand per residential customer in Florida

Based on these variables, NPP is calculated as plotted in Figure 11. In AC-PV module, the NPP is decided to be zero. Nonetheless, depending on regions, some utility companies might not accept zero NPP because their basic costs for delivering electricity to the neighborhood can vary. As a result of that, the optimum battery capacity is going to be less than the battery capacity determined in this article. When the cost of a PV panel and lithium-ion battery are considered, as shown in Figure 12, the optimum battery capacity per panel becomes 1.5 kWh per AC-PV module. This result also indicates that the batteries can be charged fully in 4 hours. Another result of this optimization is to discover the optimum inverter size if a three-port microinverter (0.4 kW) is not utilized. It can be said that 3.51 kW inverter and 13.5 kWh battery pack could be a good choice in Orlando for grid-tied PV systems where their energy usage is 1,100 kWh/month for an average household.

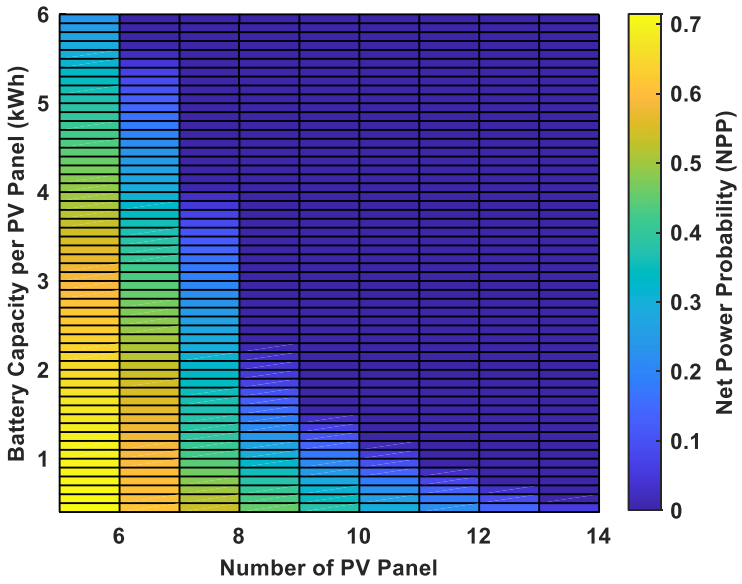

Figure 11. Net power probability distribution with a PV panel vs Battery capacity

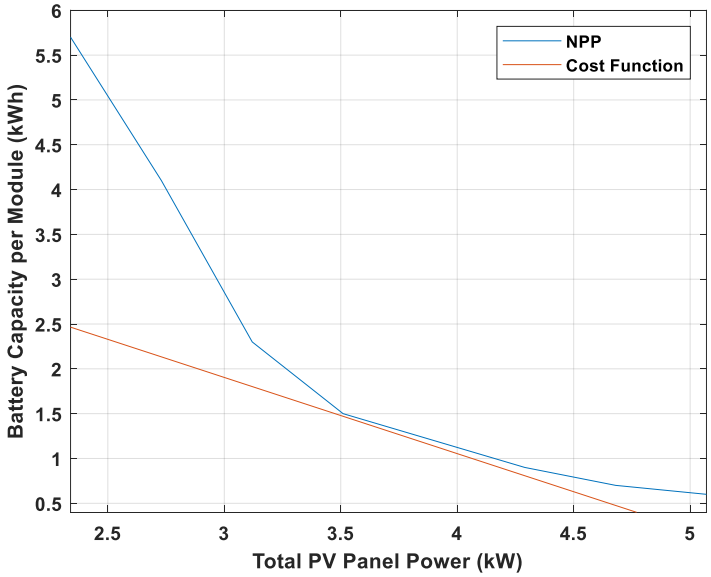

Figure 12. Determination of PV panel power and battery capacity

3.2. Determination of Battery Electrical Model Parameters

In order to find the battery electrical model parameters in Equation 3, two tests are performed. They are the pulse-relaxation test and open-circuit voltage test as illustrated in Figure 13 and 14.

When there is not electric current flowing in the module, the voltage at the terminal of a battery is equal to its open-circuit voltage. However, when the battery is either charged or discharged at a constant rate of the 1C rate, the current remains constant, and as a result, the terminal voltage decreases from the open-circuit voltage. This decrease in voltage is due to a voltage drop occurring across both the internal resistance and the parallel RC circuit. Internal resistance can be found when the discharge current ends. In Equation 3, the time "t" is 300 seconds because the battery is discharged for 5 minutes and relaxed for 3 hours. Then, Equation 25 is ultimately derived from Equation 3.

$$V_T(t) = V_{OC} - I_T \cdot R_{in} - \left(1 - e^{-\frac{300}{\tau_P}}\right) \cdot I_T \cdot R_P \tag{25}$$

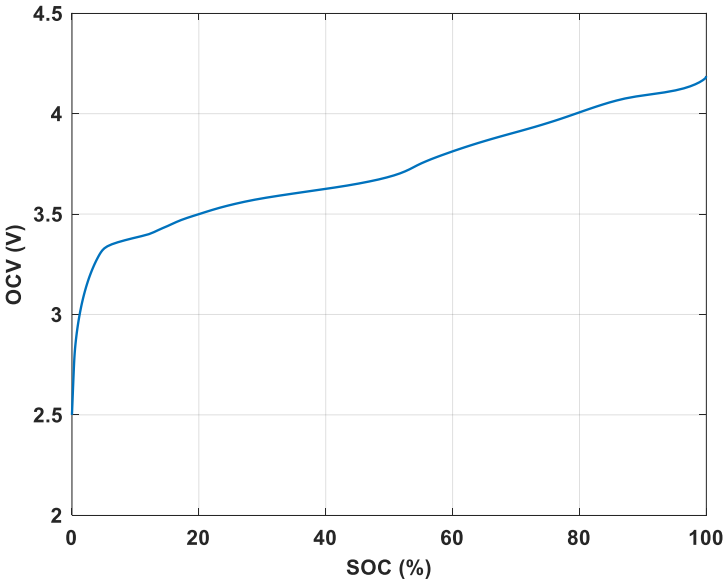

Figure 13. Open circuit voltage test

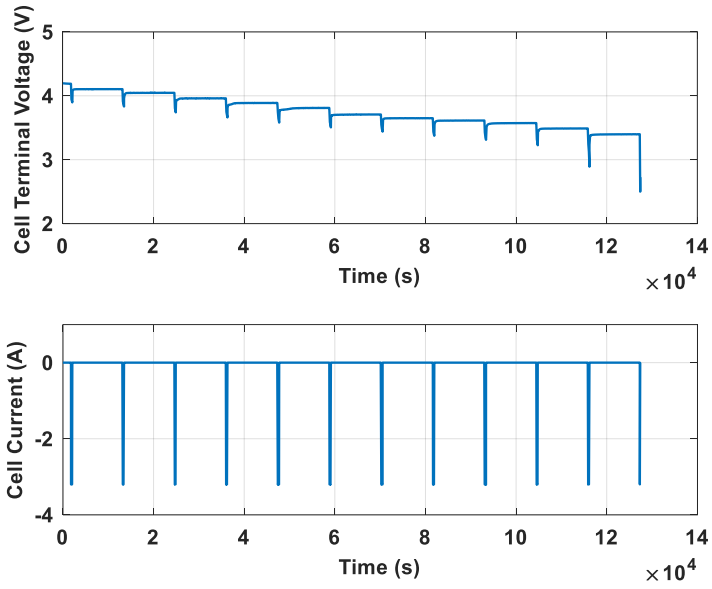

Figure 14. Pulse relaxation test during discharge at 25 Celsius

The time constant of the parallel RC circuits is 100 seconds since it corresponds to the electrolyte polarization time [24]. For example, for the discharging scenario, the average internal resistance and the average resistance in the parallel RC circuit at 25^0 C are 40.56 mΩ and 35.02 mΩ, respectively. The average internal resistance and the average resistance in the parallel RC circuit are 39.39 mΩ and 40.27 mΩ at 25^0 C for the charging scenario, respectively. They are plotted in Figure 15 and Figure 16.

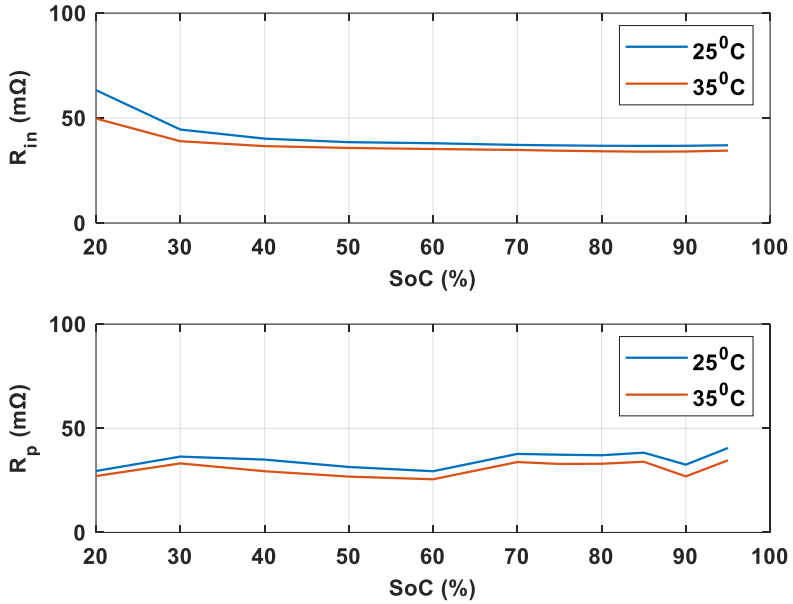

Figure 15. Internal and polarization resistance during discharge

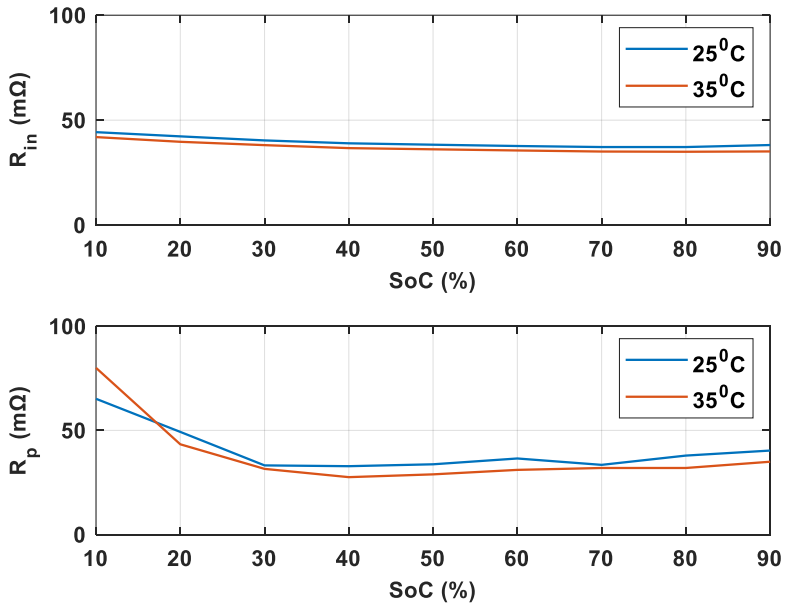

Figure 16. Internal and polarization resistance during charge

3.3. Determination of PV Temperature Model Parameters

In Equation 13, the heat flux ratio (α) of radiation to convection is evaluated at different PV panel temperatures. It is 0.62 in summer and 0.46 in winter [19]. The PV panel temperature is calculated based on the data from NREL for the Orlando area. They are the solar irradiation, the wind speed, and the weather temperature, as plotted in Figure 9, Figure 17, and Figure 18, respectively. The

solar irradiance absorption rate for chosen PV panel is 0.46, and the photoelectric efficiency of the solar cell is 0.15. As a result, the PV panel temperature does not exceed 90^0 C, as simulated in Figure 19.

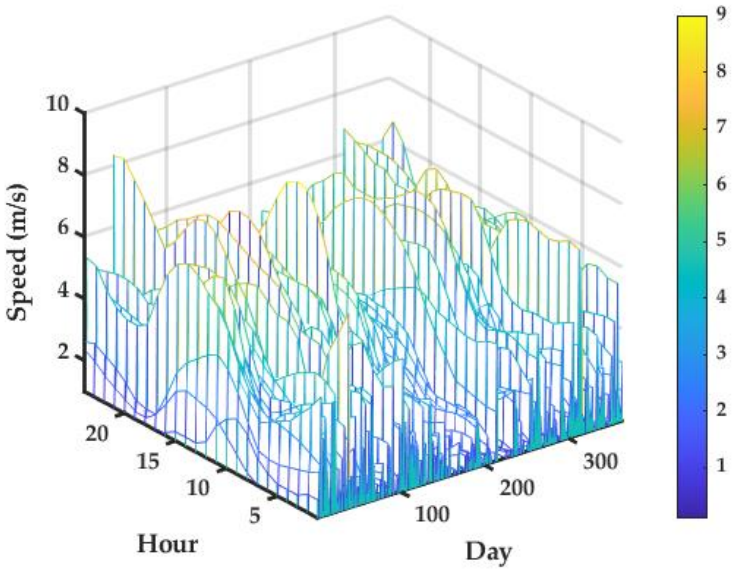

Figure 17. Wind speed in Orlando for a year

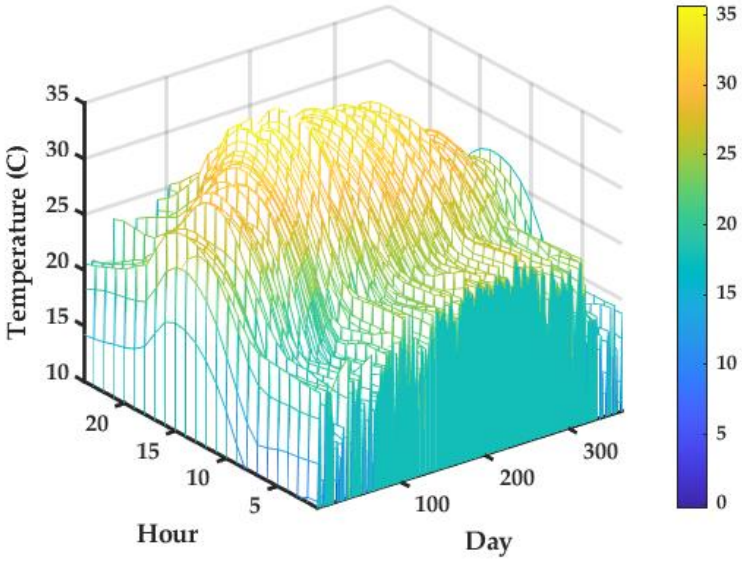

Figure 18. Weather temperature in Orlando for a year

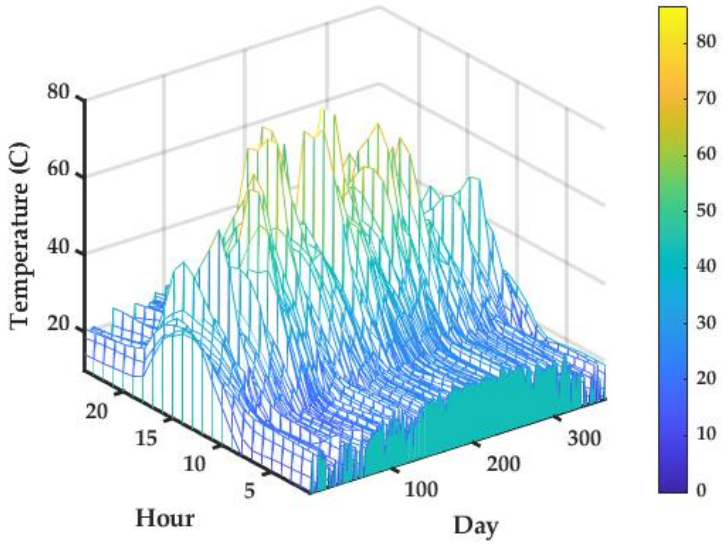

Figure 19. Estimated PV panel Temperature in Orlando for a year.

3.4. Control Algorithm Determination

US Department of Labor, Occupational Safety and Health Administration considers 50 volts and above to be hazardous [31]. Also, Energized work above 50 volts at Oak National Laboratory requires Energized Electrical Work Permit [32]. Therefore, LG 3.2 Ah battery specifications in Table 2, the battery pack voltage is lower than 50 volts (13 cells in series and 10 cells in parallel).

Table 2. Specifications of LG MH1 18650 Rechargeable Lithium Ion Battery

Item	Condition	Specification
Nominal Voltage	Average	3.67 V
Standard charge	Constant current	1550 mA
Standard charge	End current	50 mA
Standard charge	Constant voltage	4.2 V
Maximum charge	Current	3100 mA
Maximum charge	Voltage	4.205 V
Standard discharge	Constant current	620 mA
Standard discharge	End voltage	2.5 V
Maximum discharge	Current	10 A
Operating temperature	Charge	0 ~ 45 ^{o}C
Operating temperature	Discharge	-20 ~ 60 ^{o}C

As a result, the control algorithm that extracts the information of the battery pack is illustrated in Figure 20. They are the temperature, current, voltage, SoC, and SoH that are sent to the second level controller.

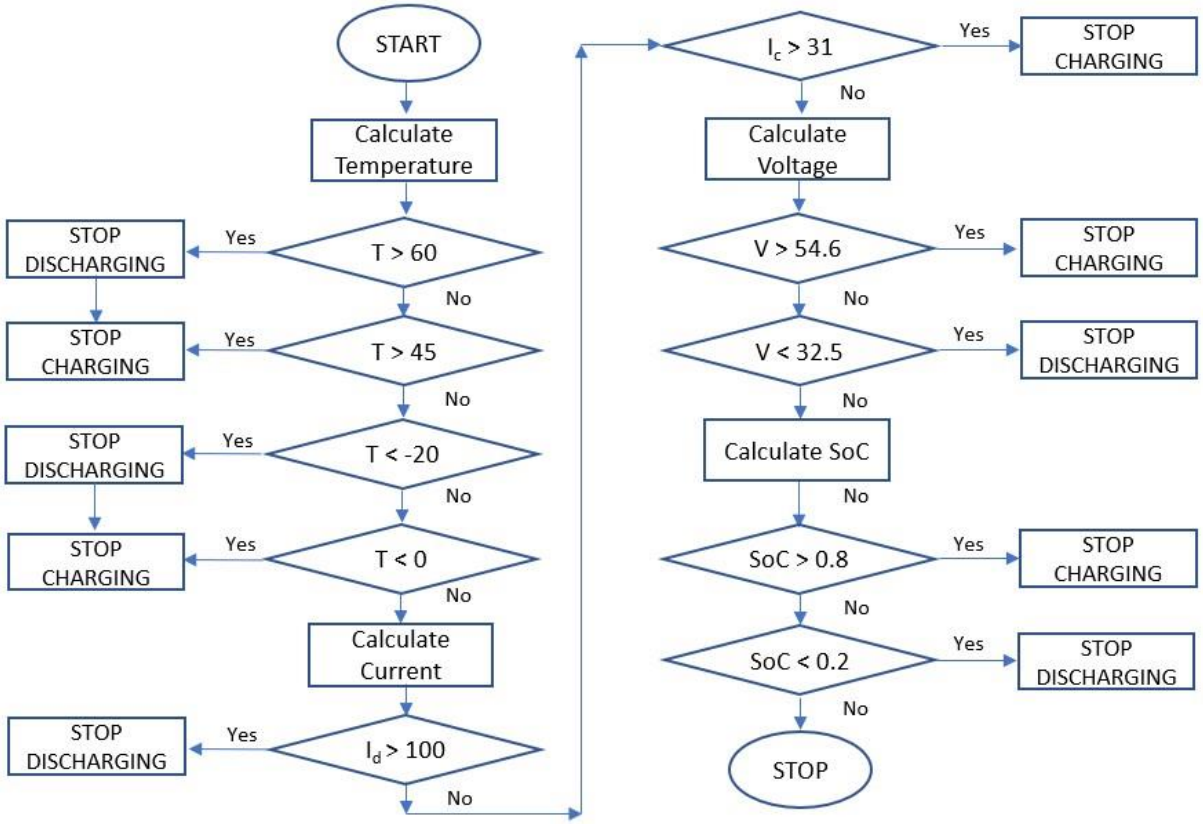

Figure 20. Control algorithm of acquiring the battery pack information

4. CONCLUSION

The article proposes the design of AC-PV module and discusses its optimization by providing simulation and test results. The goal of the proposed i-BMS is to optimize the AC-PV module to be safer, more reliable, and cost-effective. The paper demonstrates the feasibility of the AC-PV system. First of all, the battery electrical model is described and theoretically explained. Then, this battery model parameters are experimentally identified with the help of the open circuit voltage test and the pulse relaxation test. The PV panel temperature model is theoretically discussed and simulated in Orlando, Florida. It is discovered that the PV panel temperature does not exceed 90 degree Celsius. Therefore, PCM is decided as a passive thermal management system for the AC-PV module due to its weight, cost, and efficiency. Second of all, the capacity of the battery pack is estimated to be 1.5 kWh for each PV panel with 0.39 kW power rating. During the estimation process, eight different cases are encoded. Lastly, the thermal model of a battery cell is

theoretically explained to generate the on-board cells' temperature. Therefore, the one of the contribution of the AC-PV module is to use a BTMS modelling by combining two estimation methods (the Open Circuit Voltage and Coulomb Counting techniques) and a thermal management technique. Another benefit is to create a thermal map of battery module by providing each cell temperature and the AC-PV module temperature. The AC-PV module presents low installation cost, monitored and reliable i-BMS, which is applicable for residential and commercial use. It can be said that the AC-PV module may benefit one billion people who are in need of electricity.

NOMENCLATURE

PV : Photovoltaic
GFM : Grid-forming
GFL : Grid-following
IBR : Inverter Based Resources
BMS : Battery Management System
BTMS : Battery and Thermal Management System
SoC : State-of-Charge
SoH : State-of-Health
i-BMS : Intellegent Batttery Management System
ECM : Equavilent Circuit Model
PCM : Phase Change Material
PCC : Phase Change Composite
NPP : Net Power Probability

DECLARATION OF ETHICAL STANDARDS

The authors of the paper submitted declare that nothing which is necessary for achieving the paper requires ethical committee and/or legal-special permissions.

CONTRIBUTION OF THE AUTHORS

Sahin Gullu: Investigation, Methodology, Writing-Original draft, Software, Simulation, Validation and Reviewing.

Issa Batarseh: Conceptualization, Funding acquisition, Supervision and Reviewing.

Fahad Alaql: Software, Reviewing and Editing.

CONFLICT OF INTEREST

There is no conflict of interest in this study.

REFERENCES

[1] "Empower A Billion Lives," IEEE, [Online]. Available: https://empowerabillionlives.org/. [Accessed 25 January 2024].

[2] Rathnayake DB. Grid Forming Inverter Modeling, Control, and Applications, IEEE Access 2021; 9:114781-114807.

[3] Rezaei MH, Akhbari M. Power decoupling capability with PR controller for Micro-Inverter applications. International Journal of Electrical Power & Energy Systems 2022;136.

[4] Rezaei MH, Akhbari M. An active parallel power decoupling circuit with a dual loop control scheme for micro-inverters. International Journal of Electrical Power & Energy Systems 2021;49 (12): 3994-4011.

[5] Alluhaybi K, Haibing H, Batarseh I. Design and Implementation of Dual-input Microinverter for PV-Battery Applications. IEEE Applied Power Electronics Conference and Exposition (APEC). IEEE, 2020.

[6] Vega-Garita, L. Ramirez-Elizondo, Bauer P. Physical integration of a photovoltaic-battery system: A thermal analysis. Applied Energy 2017;208: 446-455.

[7] Duryea S, Islam S, Lawrance W.A battery management system for standalone photovoltaic energy systems, Conference Record of the IEEE Industry Applications Conference. Thirty-Fourth IAS Annual Meeting 1999;4:2649-2654, .

[8] Cheng KWE, Divakar BP, Wu H, Ding K, Ho HF. Battery-Management System (BMS) and SOC Development for Electrical Vehicles. in IEEE Transactions on Vehicular Technology 2011;60: 76-88.

[9] Ghosh S, Barman JC, Batarseh I, Model Predictive Control of Multi-input Solar-Wind Hybrid System in DC Community with Battery Back-up, 2021 IEEE 12th International Symposium on Power Electronics for Distributed Generation Systems (PEDG), 2021: 1-8.

[10] Xiong R, Li L, Tian J, Towards a smarter battery management system: A critical review on battery state of health monitoring methods. Journal of Power Sources 2018; 405: 18-29.

[11] Ali MU, Zafar A, Nengroo SH, Hussain S, Alvi MJ, Kim HJ. Towards a Smarter Battery Management System for Electric Vehicle Applications: A Critical Review of Lithium-Ion Battery State of Charge Estimation. Energies 2019; 12 (3): 446.

[12] Ren H, Zhao Y, Chen S, Wang T. Design and implementation of a battery management system with active charge balance based on the SOC and SOH online estimation. Energy 2019; 166: 908-917.

[13] Rezaii R, Ghosh S, Safayatullah M, Milad Tayebi S, Batarseh I. Quad-Input Single-Resonant Tank LLC Converter for PV Applications. IEEE Transactions on Industry Applications 2023; 59 (3) 3438-3457.

[14] Nilian M, Rezaii R, Safayatullah M, Gullu S, Alaql F, Batarseh I. A Three-port Dual Active Bridge Resonant Based with DC/AC Output, 2023 IEEE Energy Conversion Congress and Exposition (ECCE), Nashville, TN, USA, 2023. (Accepted)

[15] Rezaii R. Design and Implementation of a Multiport System for Solar EV Applications," 2023 IEEE Applied Power Electronics Conference and Exposition (APEC), Orlando, FL, USA, 2023, pp. 29-34.

[16] Rezaii R, Ghosh S, Safayatullah M, I. Batarseh. Design and Implementation of a Five-Port LLC Converter for PV Applications. 2023 IEEE Applied Power Electronics Conference and Exposition (APEC), Orlando, FL, USA, 2023.

[17] Gullu S, Phelps J, Batarseh I, Alluhaybi K, Salameh M. and Al-Hallaj S, Smart Battery Management System for Integrated PV, Microinverter and Energy Storage. 12th International Renewable Energy Congress (IREC), 2021.

[18] Xiong R. Battery Management Algorithm for Electrical Vehicles, Springer & China Machine Press, Singapore, 2020.

[19] Du Y, Fell CJ, Duck B, Chen D, Liffman K, Zhang Y, Gu M, Zhu Y. Evaluation of photovoltaic panel temperature in realistic scenarios. Energy Conversion and Management 2016; 108:60-67.

[20] Yang S, Ling C, Fan Y, Yang Y, Tan X, Dong H. A Review of Lithium-Ion Battery Thermal Management System Strategies and the Evaluate Criteria. International Journal of Electrochemical Sciences 2019; 14: 6077-6107.

[21] Al-Zareer M, Dincer I, Rosen MA. A novel approach for performance improvement of liquid to vapor based battery cooling systems. Energy Conversion and Management 2019; 187: 191-204.

[22] Lu M, Zhang X, Ji J, Xu X, Zhang Y. Research progress on power battery cooling technology for electric vehicles. Journal of Energy Storage 2020; 27.

[23] Feng L. et al. Experimental investigation of thermal and strain management for lithium-ion battery pack in heat pipe cooling. Journal of Energy Storage2018; 16: 84-92.

[24] Salameh M, Wilke S, Schweitzer B, Sveum P, Al-Hallaj S, Krishnamurthy M, Thermal State of Charge Estimation in Phase Change Composites for Passively Cooled Lithium-Ion Battery Packs. IEEE Transactions on Industry Applications 2018; 54(1): 426-436.

[25] Schuler K. (2021, 1 20). Retrieved from MEDILL Reports Chicago: https://news.medill.northwestern.edu/chicago/chicago-company-makes-batteries-cool-again/.

[26] Chen C, Plunkett S, Salameh M, Stoyanov S, Al-Hallaj S, Krishnamurthy M. Enhancing the Fast-Charging Capability of High-Energy-Density Lithium-Ion Batteries: A Pack Design Perspective. IEEE Electrification Magazine 2020; 8(3): 62-69.

[27] Ali HM. Recent advancements in PV cooling and efficiency enhancement integrating phase change materials-based systems – A comprehensive review. Solar Energy 2020; 197: 163-198.

[28] AllCell Technologies (www.allcelltech.com)

[29] Cole W, Frazier AW, Augustine C. Cost Projections for Utility-Scale Battery Storage: 2021 Update. National Renewable Energy Laboratory, NREL/TP-6A20-79236, Golden, CO, 2021.

[30] Feldman D, Ramasamy V, Fu R, Ramdas A, Desai J, Margolis R. U.S. Solar Photovoltaic System Cost Benchmark: Q1. National Renewable Energy Laboratory, NREL/TP-6A20-77324, Golden, CO, 2021.

[31] Occupational Safety and Health Administration, U.S. Department of Labor, [Online]. Available: https://www.osha.gov/laws-regs/standardinterpretations/2015-09-04#:~:text=However%2C%20OSHA%20considers%20all%20voltages,the%20resistance%20of%20the%20object. [Accessed 25 January 2024].

[32] Harter J, McIntyre TJ, White JD. Electrical Safety Practices Developed for Automotive Lithium-Ion Battery Dismantlement. Oak Ridge National Laboratory, ORNL/TM-2019/1366, Oak Ridge, TN, 2020.